# Conjugated Polyene Fatty Acids as Fluorescent Probes: Binding to Bovine Serum Albumin†

Larry A. Sklar,‡ Bruce S. Hudson,*,§ and Robert D. Simoni¶

ABSTRACT: The binding of the conjugated polyene fatty acids, *cis*-parinaric acid (9,11,13,15-*cis,trans,trans,cis*-octadecatetraenoic acid) and *cis*-eleostearic acid (9,11,13-*cis,trans,trans*-octadecatrienoic acid), to bovine serum albumin has been studied by using absorption and fluorescence properties of the polyene chromophores. These studies demonstrate the utility of polyene fatty acids as probes of lipid–protein interactions. Shifts in the absorption spectrum, enhancement of parinaric acid fluorescence, induced circular dichroism in the polyene chromophore, and energy transfer between the tryptophan residues and the bound chromophores all provide information about the binding of these fatty acids to albumin. Strong reversible binding of parinaric acid and eleostearic acid to bovine serum albumin is observed. Fluorescence and absorption measurements demonstrate that there are binding sites for approximately five fatty acid molecules with binding constants $\sim 10^6$ to $10^8$ $M^{-1}$, similar to previous results for oleic acid. An induced circular dichroism arises when the polyene is bound to approximately four of these tightest binding sites. This circular dichroism is complex when more than one parinaric acid molecule is bound to the protein and is attributed to excitonic ligand–ligand interactions. Fluorescence quenching of the albumin tryptophan residues by parinaric acid is more efficient than quenching by eleostearic acid, consistent with expectations for singlet–singlet Förster transfer. The availability of two homologous polyene fatty acids with very different spectral overlap integrals with tryptophan enhances the reliability of intramolecular distance determinations by the energy transfer technique. A procedure is given for the decomposition of the total energy transfer efficiency into the contributions for each of the two tryptophan donors.

Biological membranes are complex assemblies of lipid and protein molecules. Substantial evidence indicates that the function and conformation of many membrane proteins are dependent upon association with lipids and on the lipid physical state.[1] A detailed understanding of the structure and function of biological membranes requires the elucidation of the nature and extent of lipid–protein interactions.

We have recently demonstrated that conjugated polyene fatty acids are useful probes of membrane structure (Sklar et al., 1975, 1976). *cis*-Parinaric acid (9,11,13,15-*cis,trans,trans,cis*-octadecatetraenoic acid) and *cis*-eleostearic acid (9,11,13-*cis,trans,trans*-octadecatrienoic acid) have been spectroscopically characterized (Sklar et al., 1977a) and the response of these chromophores and linear polyenes in general to environmental parameters is well understood (Hudson and Kohler, 1974). We have characterized the use of parinaric acid as a fluorescent probe of synthetic phospholipid membranes (Sklar et al., 1977b). These studies have emphasized the similarity of these fatty acid probe molecules to normal membrane components and the minimal perturbing influences that they should exert.

This paper reports the use of polyene fatty acids to examine lipid–protein interactions. We have examined the reversible binding of *cis*-parinaric acid to bovine serum albumin (BSA[2]). BSA is well suited to these initial studies since it has been extensively characterized. BSA has a molecular weight of 69 000 and contains 2 tryptophan and 20 tyrosine residues (Longworth, 1971). A prime physiological role of the protein is as a carrier of free fatty acids in serum. Several investigators have concluded that a total of 5 to 6 mol of long-chain fatty acid bind per mol of albumin with binding constants in the range of $10^6$ to $10^8$ $M^{-1}$ (Spector, 1975), and that there are several additional binding sites of lower affinity. One of the tryptophan residues is thought to reside near a site of high fatty acid binding affinity. Recent sequence studies of mammalian albumins, including BSA, have revealed a pattern of internal homology and disulfide bridges from which a structural organization model has been deduced (Brown, 1976).

Spectroscopic analysis of the binding of long-chain ligands to bovine serum albumin has been extensive (see review by Spector, 1975). Measurement of the ligand binding usually requires a two-phase partition technique (Goodman, 1958), particularly in the case of long-chain fatty acids (Spector, 1975). Several types of long-chain probe molecules including nitroxide-labeled fatty acids (Morrisett et al., 1975) and trifluoroalkyl sulfate ions (Muller and Mead, 1973) have also been used, but there remains some uncertainty concerning the binding specificity of these molecules and the effects that detergent-like molecules have on the conformation of this protein (Reynolds et al., 1968). It appears therefore that conclusions about fatty acid binding obtained with ligands other than natural fatty acids should be viewed with caution. The work presented here represents a synthesis of the two approaches since the probe molecule is itself a long chain fatty acid.

In preliminary studies (Sklar et al., 1975, 1976) we have shown that parinaric acid binds to BSA and is an energy

† From the Departments of Chemistry and Biological Sciences, Stanford University, Stanford, California 94305. *Received January 1, 1977; revised manuscript received July 13, 1977.* This work was supported by the National Institutes of Health (Grants GM 21149 and EY 01518 to B.S.H. and GM 18539 to R.D.S.) and a grant from the Research Corporation to B.S.H.

‡ Taken in part from the thesis submitted by L.A.S. in partial fulfillment of the Ph.D. requirements, Stanford University (1976). Present address: Division of Atherosclerosis and Lipoprotein Research, Department of Medicine, The Methodist Hospital, Baylor College of Medicine, Houston, Tex. 77025. L.A.S. is a Helen Hay Whitney Postdoctoral Fellow.

§ Camille and Henry Dreyfus Teacher-Scholar and Alfred P. Sloan Fellow.

¶ Department of Biological Sciences, Stanford University.

[1] For recent reviews, see: (1976), The Enzymes of Biological Membranes, Vol. 1, Martonosi, A., Ed., New York, N.Y., Plenum Press; (1975), Biomembranes: Lipids, Proteins and Receptors, Burton, R. M., and Packer, K., Ed., Webster Groves, Mo., BI-Science; Singer, S. J. (1974), *Annu. Rev. Biochem. 45*, 805–833.

[2] Abbreviations used are: BSA, bovine serum albumin; *cis*-PnA, *cis*-parinaric acid; *cis*-EsA, *cis*-eleostearic acid; CD, circular dichroism; DMPOPOP, 1,4-bis[2-(4-methyl-5-phenyloxazolyl)]benzene.

transfer acceptor of tryptophan fluorescence emission. In this report, we describe how the interaction of *cis*-parinaric and *cis*-eleostearic acid with albumin may be monitored by several spectroscopic techniques: absorption spectrum and fluorescence quantum yield changes, induced circular dichroism, and energy transfer between tryptophan residues and bound probe.

## Materials and Methods

*Serum Albumin.* Bovine serum albumin (BSA), crystallized and lyophilized and essentially fatty acid free (less than 0.005%, or 0.02 fatty acid per BSA), was obtained from Sigma Chemical Co. (Lot 93V-7-10) and was used without further purification. Polyacrylamide gel electrophoresis shows this preparation to be free of major impurities. The occurrence of BSA dimers and higher oligomers in equilibrium with monomers has been discussed elsewhere (Morrisett et al., 1975), where it was reported not to affect fatty acid binding. Solutions of BSA were prepared in 0.01 M potassium phosphate buffer, pH 7.4, and used within 24 h.

*Fatty Acids. cis*-Parinaric acid (9,11,13,15-*cis,trans,-trans,cis*-octadecatetraenoic acid) and *cis*-eleostearic acid (9,11,13-*cis,trans,trans*-octadecatrienoic acid) were prepared as described previously (Sklar et al., 1977b) and were greater than 99% pure. *cis*- and *trans*-parinaric acid are commercially available from Molecular Probes, Roseville, Minn. Oleic acid (99%) was obtained from Calbiochem. Ethanolic solutions of the polyene fatty acids ($\sim 4 \times 10^{-3}$ M) were used for addition to aqueous albumin solutions. The final concentration of ethanol in the solution did not exceed 0.1% (v/v) and had no effect on the measurements. Solutions used for spectroscopic measurements have been purged with argon and contained small amounts of antioxidant. These precautions ensure negligible polyene decomposition.

*Spectroscopic Measurements.* Absorption spectra were recorded on a Cary 14 scanning spectrophotometer whose wavelength calibration had been compared with the emission lines of a low-pressure mercury lamp. Repetitive determinations indicate that polyene absorption maxima may be reproducibly measured to within 0.2 nm. Fluorescence measurements were recorded on a Hitachi Perkin-Elmer MPF-2A spectrofluorimeter. Quantum yields were measured using DMPOPOP in cyclohexane as a standard of $Q = 0.93$ (Sklar et al., 1977a; Berlman, 1971). Circular dichroism spectra were recorded on a Jasco J-40 spectropolarimeter.

*Energy Transfer Analysis for the Case of Multiple Donors.* For a donor–acceptor pair with a fixed relative distance and transition dipole orientation the energy transfer rate is given by

$$k_{da} = 8.71 \times 10^{23} n^{-4} Q_d k_D J_{da} (\kappa_{da}^2 / R_{da}^6) \qquad (1)$$

where $Q_d$ is the fluorescence quantum yield and $k_D$ (in $s^{-1}$) is the excited state decay constant of donor d in the absence of any acceptors, $J_{da}$ is the donor–acceptor spectral overlap integral ($cm^3\ M^{-1}$), $n$ is the refractive index of the medium surrounding the chromophores, $\kappa^2$ is the dipole–dipole orientation factor, and $R_{da}$ is the donor–acceptor distance (Å). The total rate of decay of the excitation of donor d is given by

$$1/\tau = k_D + \sum_{a=1}^{\nu} k_{da} \equiv k_D + K_d \qquad (2)$$

where $K_d$ is the sum of the energy transfer rates for the donor to all acceptors. ($K_d$ is a function of the number of acceptors $\nu$ which ranges from 1 to 5 in our experiments.) The energy transfer efficiency for donor d is given by

$$T_d^A = K_d/(k_D + K_d) \qquad (3)$$

The measured transfer efficiency is the weighted sum over the $\mu$ donors

$$\overline{T}^A = \sum_{d=1}^{\mu} f_d T_d^A \qquad (4)$$

where $f_d$ is the fraction of the fluorescence contributed by donor d in the absence of transfer to the acceptors. Combining eq 1-3 yields

$$[(1/T) - 1]^{-1} = J_d^A [8.71 \times 10^{23} n^{-4} Q_d \sum_{a=1}^{\nu} (\kappa_{da}^2/R_{da}^6)] \qquad (5)$$

where it has been assumed that all of the acceptors are of the same type (designated A) with the same absorption spectrum, i.e., $\nu$ spectrally identical acceptors.

The special case of interest in this work is the situation where there are two fluorescent donors ($\mu = 2$ in eq 4). The objective of this analysis is the decomposition of the observed total transfer efficiency into the contributions due to each donor. In other words, we would like to know whether all of the quenching is due to transfer from one donor to neighboring acceptors or whether partial quenching occurs for both donors. Measurement of the total transfer efficiency as a function of the number of acceptors of a given type does not yield enough information for the determination of the individual transfer efficiencies.

The necessary additional information can be obtained by performing independent experiments with two or more structurally analogous acceptors which are spectrally distinct. By "structurally analogous" we mean that the quantity in square brackets in eq 5 is the same for both types of acceptors for a given value of $\nu$. By "spectrally distinct" we mean that the spectral overlap integral is different for the two acceptors. Under these conditions we have

$$[(1/T_d^A) - 1] = [(1/T_d^B) - 1]\Gamma_d \qquad (6)$$

where $\Gamma_d \equiv J_d^B/J_d^A$ is the ratio of the spectral overlap integrals for donor d to acceptors of type A or B. This equation may be written for each donor. For the case of two donors it provides two relations between the four unknowns $T_I^A$, $T_{II}^A$, $T_I^B$, and $T_{II}^B$. Two further relations are provided by eq 4 since this equation may be written for each type of acceptor.

$$\overline{T}^x = f_I T_I^x + (1 - f_I) T_{II}^x \qquad (7)$$

$\overline{T}^x$ is the measured total transfer efficiency in the presence of acceptors of type $x$. A simplified notation leads to the following set of equations

$$\begin{aligned} as + (1-a)t &= b \\ au + (1-a)v &= c \\ [(1/s) - 1] &= [(1/u) - 1]d \\ [(1/t) - 1] &= [(1/v) - 1]e \end{aligned} \qquad (8)$$

where $a = f_I$, $b = \overline{T}^A$, $c = \overline{T}^B$, $d = \Gamma_I$, $e = \Gamma_{II}$, $s = T_I^A$, $t = T_{II}^A$, $u = T_I^B$, and $v = T_{II}^B$. The first five quantities are considered to be known and $s$, $t$, $u$, and $v$ are unknown. This system of equations reduces to a quadratic equation.

$$As^2 + Bs + C = 0 \qquad (9)$$

where

$$\begin{aligned} A &\equiv a(d-e) + c(1-d)(1-e) + (1-d)e \\ B &\equiv (1-a)(d-e) - b(d-e) - c[(1-e) + (1-d)] \\ &\quad + c(1-d)/a - cb(1-d)(1-e)/a - be(1-d)/a \\ C &\equiv [cb(1-e) + eb(1-e) - c(1-a)]/a \end{aligned} \qquad (10)$$

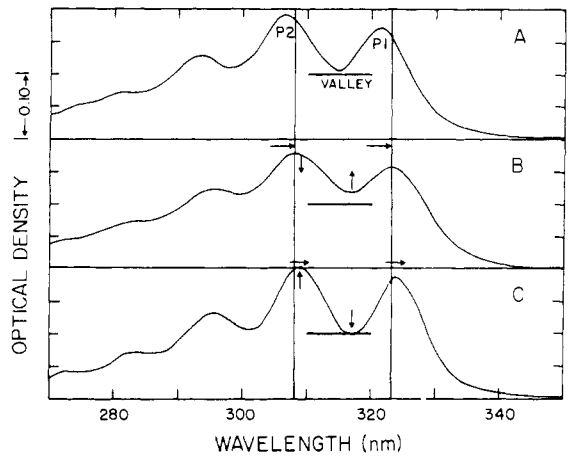


FIGURE 1: The absorption spectrum of *cis*-PnA in the presence of various amounts of BSA. The concentration of *cis*-PnA is $3.65 \times 10^{-6}$ M. The sample in A contains *cis*-PnA alone (no mol of BSA/mol of PnA). The sample in B contains 0.12 mol of BSA/mol of PnA. The sample in C contains 1 mol of BSA/mol of PnA.

Solution of eq 9 results in a separation of the observed total transfer efficiency into the components due to the individual donors subject to the assumption that the two spectrally distinct types of acceptors are structurally similar.

## Results and Discussion

*Binding of Polyene Fatty Acids by Absorption Spectroscopy.* The absorption spectra of *cis*-parinaric acid (*cis*-PnA) in aqueous solutions with increasing BSA concentration are shown in Figure 1. The concentration of *cis*-PnA is approximately $4 \times 10^{-6}$ M in each case. The spectrum in buffer, without BSA, is shown in Figure 1A. The first absorption peak, P1, is located at 321 nm, and the value of the ratio of the extinction coefficient at the first minimum "valley" to its value at the second peak (P2) is 0.52. Solvent studies indicate that the position of P1 can vary between about 318 and 326 nm, depending upon the solvent polarizability, and that the value of the ratio of the extinction coefficient at the "valley" to that at P2 ($V/P$) is typically in the range of 0.45 to 0.52 for *cis*-PnA dissolved in pure solvents (Sklar et al., 1977a). The spectrum shown in Figure 1B results when 0.12 mol of albumin is added per mol of *cis*-PnA. The arrows indicate the direction of small but reproducible shifts in the absorption spectrum. P1 shifts to about 323 nm, and the value of $V/P$ is a maximum, 0.65. The spectrum in Figure 1C is obtained when 1 mol of albumin is present per mol of *cis*-PnA. The spectrum is sharpened considerably, P1 is near 324 nm and $V/P$ is 0.48. These final values do not change as further albumin is added, indicating that nearly all of the *cis*-PnA is bound under these conditions. For comparison, at the same concentrations 99% of oleic acid is bound to BSA (Spector et al., 1971).

Since P1 of the aqueous spectrum is located near the valley of the bound spectrum, the $V/P$ ratio (a measure of the "sharpness" of the spectrum) is a sensitive indicator of the multiplicity of species present. If the observed spectrum results from only two components (i.e., free and bound), and the spectra of those two components have similar extinction coefficients differing only in the location of the absorption maxima, then the value of $V/P$ will be a maximum when the concentrations of the species are approximately equal.

An analysis of the shifts of the absorption spectrum of *cis*-PnA in response to binding to albumin is shown in Figure 2. Figure 2A shows $V/P$ as a function of the molar ratio of BSA to *cis*-PnA. This spectral ratio is a maximum near 0.10 to 0.12

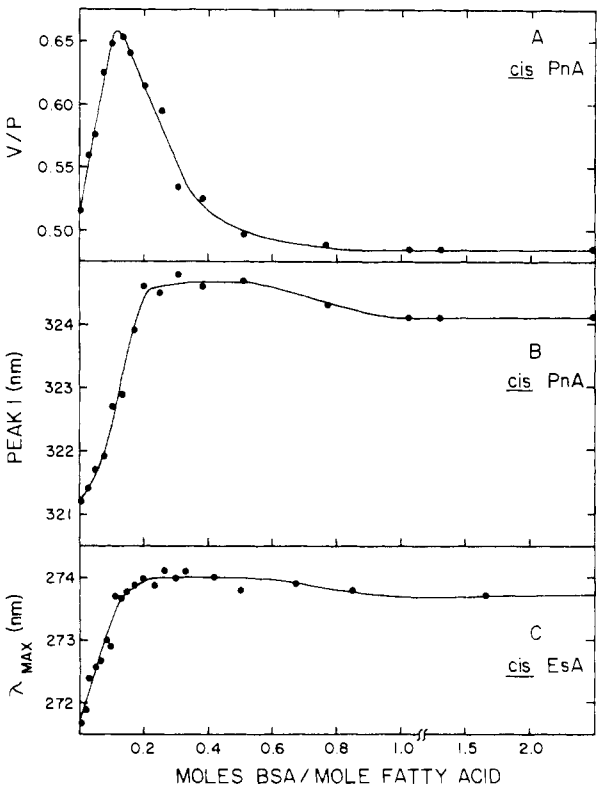


FIGURE 2: The changes in the absorption spectra of *cis*-PnA and *cis*-EsA upon binding to BSA. (A) The ratio of the optical density of the valley, $V$, to the optical density of peak 2 (see Figure 1A). (B) The absorption peak position of peak 1, of *cis*-PnA. (C) The absorption maximum of *cis*-EsA (see Figure 6). The concentrations of both *cis*-PnA and *cis*-EsA were $3.65 \times 10^{-6}$ M. BSA was added as microliter aliquots to sample and reference cuvettes from a stock solution.

mol of BSA per mol of *cis*-PnA (or 8 to 10 *cis*-PnA per BSA) and indicates that roughly half, or approximately 4 to 5 mol of *cis*-PnA, is bound per mol of BSA. In addition, the location of the absorption maximum P1 as a function of the amount of BSA is shown in Figure 2B. The peak shift is monotonic from 321.2 nm (in the absence of BSA) and reaches a maximum value of 324.6 nm at the ratio of 0.3 mol of BSA per mol of PnA. The shift is halfway between these limits at a ratio of 0.1 mol of BSA per mol of *cis*-PnA which indicates that free and bound species contribute equally to the spectrum at this mole ratio and concentration. However, as the ratio of BSA per *cis*-PnA approaches 1, the position of P1 shifts back to 324.2 nm. Circular dichroism results discussed below suggest that this may be related to excitonic interactions between the parinaric acid ligands that occur only when more than 1 *cis*-PnA is bound per BSA.

BSA has similar binding properties for *cis*-PnA, *cis*-EsA, and oleic acid. This result is anticipated due to the similarity in the overall shape and dimensions of these molecules, as previously discussed (Sklar et al., 1975). Each of these fatty acids is 18 carbons in length and contains a $\Delta^9$-cis bond. Since the absorption spectrum of *cis*-eleostearic acid is not sharp (see Figure 6), it is difficult to measure $V/P$. Figure 2C shows the location of the absorption maximum for a solution of eleostearic acid as BSA is added in a series of experiments similar to the ones described for *cis*-PnA in Figures 1 and 2. The shifts correlate quite well with those observed for *cis*-PnA. In particular, a maximum shift occurs when about 0.3 mol of BSA is present per *cis*-EsA, and a slight decrease in the wavelength of P1 occurs as the concentration ratio approaches 1.

The binding experiments described have been carried out

at constant *cis*-PnA concentration. Direct absorption and difference spectral studies performed at constant BSA concentration are complementary to these studies. A discussion of the results appears elsewhere (Sklar, 1976). These studies support the contention that 5 mol of *cis*-PnA bind tightly to BSA at these concentrations. Difference spectral studies permit the observation of the distribution of successive amounts of *cis*-PnA as the protein binding sites saturate. Competitive binding experiments between oleic acid and parinaric acid for BSA binding sites (Sklar, 1976) using absorption spectroscopy confirm that the binding affinity of these fatty acids is very similar, that the binding is reversible, and that the same sites are involved.

*The Binding of cis-Parinaric Acid to Albumin by Enhanced Fluorescence.* The fluorescence quantum yield of *cis*-PnA in an aqueous solution is less than 0.001 compared with a value of approximately 0.04 when bound to BSA. No change in the emission spectrum, except for the enhancement, is observed. The enhancement of the fluorescence of a solution of *cis*-PnA to which albumin is added is shown in Figure 3A. This experiment is carried out under concentration conditions similar to those used for the absorption experiments of Figures 1 and 2 so that a direct comparison of the results is possible. The initial linear increase in fluorescence intensity extrapolates to a maximal value close to 0.2 mol of BSA per mol of *cis*-PnA, consistent with about five fatty acid binding sites which can be occupied at this concentration. There is no further increase in fluorescence intensity when BSA exceeds the ratio of 0.4 mol of albumin per mol of *cis*-PnA. This result is interpreted to indicate that no further binding occurs and that under these conditions only a vanishingly small amount of free *cis*-PnA remains. In contrast, beyond this molar ratio the absorption spectrum (Figure 2A,B) sharpens and is accompanied by a small peak shift, believed to be due to the reduction of ligand–ligand interactions rather than binding changes.

A Scatchard plot may be derived from the data of Figure 3A. It has been assumed that the quantum yield of bound *cis*-PnA is similar in all of the sites and that maximal fluorescence represents 100% binding. The percentage of parinaric acid bound is then given by the percentages expressed in Figure 3A. This plot is shown in Figure 3B where $\nu$ is the number of sites on the protein occupied by *cis*-PnA, and $c$ is the concentration of free *cis*-PnA (uncorrected for possible complications of fatty acid solubility phenomena (Spector, 1975)). The slope of such a plot is the binding constant, and curved plots indicate nonequivalent binding sites or site–site interactions. Data between the region of about $\nu = 3$ to 5 are obtained because of the experimental conditions. No data are obtained for the three tightest binding sites because of the assumption that maximal fluorescence was equivalent to 100% binding. This also indicates that the affinity of these tightest sites is sufficiently large that less than 1% of free *cis*-PnA remains. The fourth site has a slope (i.e., binding constant) on the order of $10^7$ $M^{-1}$ and the fifth site has a slope on the order of $3 \times 10^6$ $M^{-1}$. There are probably several additional sites of lower affinity that are not observed under the experimental conditions. The first three sites have slopes on the order of $10^7$ $M^{-1}$ or greater. This range of values for the binding of the first 5 mol of *cis*-PnA to BSA (i.e., $10^6$ to $10^8$ $M^{-1}$) is comparable to the range of values obtained for the binding of other long-chain fatty acids. Goodman (1958) analyzed fatty acid binding data in terms of classes of binding sites, with equal affinities within each class. More recently, the inadequacy of this analysis has been pointed out, and sequentially decreasing individual binding constants have been proposed (Spector et al., 1971; Ashbrook et al., 1975; Spector, 1975). Nonetheless, the evidence clearly indicates a

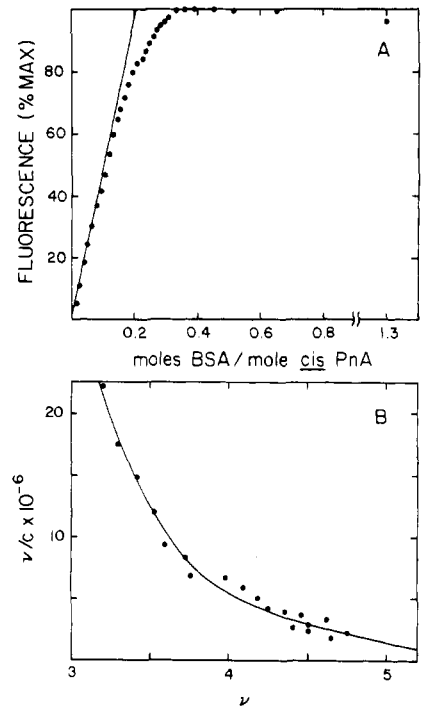


FIGURE 3: The binding of *cis*-PnA to BSA as determined by fluorescence enhancement. (A) Fluorescence intensity of *cis*-PnA. The concentration of *cis*-PnA was $3.1 \times 10^{-6}$ M. BSA was added as microliter aliquots from a stock solution. Fluorescence excitation was at 325 nm (slit 2 nm) and emission determined at 410 nm (bandwidth 40 nm). Corrections were made for the small contribution of tryptophan fluorescence. (B) A Scatchard analysis of the data presented in A. It was assumed that the maximal fluorescence achieved when a large excess of BSA was added represents 100% binding, and that the amount of *cis*-PnA bound is proportional to its relative fluorescence intensity. The concentration of free *cis*-PnA is given by $c = (1 - \%\ \text{fluorescence}/100\%)\ 3.1 \times 10^{-6}$ M. The number of moles of PnA bound per BSA is $\nu$.

similarity in the binding affinities of BSA for the polyene fatty acids and other long-chain fatty acids. Competitive fluorescence binding experiments again indicate that parinaric acid is displaced from BSA by oleic, stearic, and palmitic acid, and quantification of these results indicates that the binding affinities of oleic acid and parinaric acid are the same to within a factor of two for the first five sites.

*The Induced Circular Dichroism of cis-PnA Bound to Bovine Serum Albumin.* The circular dichroism spectrum of *cis*-PnA bound to BSA is shown in Figure 4. The contribution of BSA with bound oleic acid at the same concentration has been subtracted. On an equal molar basis the CD of albumin is negligible for wavelengths longer than 290 nm. When less than 1 mol of PnA is bound per BSA molecule, the observed CD is entirely positive. For ratios of *cis*-PnA/BSA greater than one, a complex CD is observed with a negative long wavelength component. As the ratio of *cis*-PnA/BSA increases, the negative CD component becomes larger until at a ratio of about 2.5 the spectrum is fully developed. Thus, the spectrum of a sample with a mole ratio of *cis*-PnA/BSA of 14 (not shown) has the same relative proportions of negative and positive components as does one with *cis*-PnA/BSA equal to 3.5 shown in Figure 4 (see also Figure 5).

The experimental strategy of these binding experiments involves varying the BSA concentration while maintaining the *cis*-PnA concentration constant. The results of the CD experiments are summarized in Figure 5. The molar ellipticities of the largest positive peak, the negative peak, and the sum of their absolute values is plotted vs. the molar ratio of BSA to

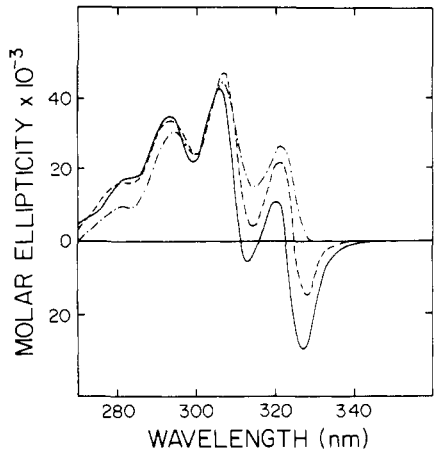


FIGURE 4: The induced circular dichroism of *cis*-PnA bound to BSA. The concentration of *cis*-PnA was $1.44 \times 10^{-5}$ M. CD spectra are shown for ratios of *cis*-PnA/BSA of 3.5/1 (—), 1.4/1 (- - -), and 0.8/1 (···), for which the contributions of the CD of BSA (containing the same ratio of oleic acid) have been subtracted.

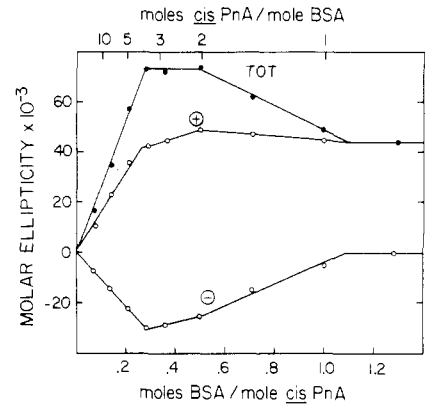


FIGURE 5: The molar ellipticities of *cis*-PnA bound to BSA. The concentration of *cis*-PnA was $1.44 \times 10^{-5}$ M. BSA was added as aliquots of a stock solution. CD spectra were recorded for each of these samples and corrected for the contribution of BSA (containing an identical ratio of mol of oleic acid/mol of BSA). The molar ellipticities of the largest positive peak, about 309 nm (+), the negative peak (−), and the sum of their absolute values (TOT) are displayed vs. the ratio of mol of *cis*-PnA/mol of BSA.

*cis*-PnA. The concentration of *cis*-PnA is about fivefold higher than the comparable absorption experiments and, by the methods described for Figures 1 and 2, a total of 6 to 7 binding sites are observed. At low molar ratios of BSA/*cis*-PnA, there is an excess of free cis-PnA. Since the free species does not contribute to the CD, the binding may be monitored by the CD measurement even in the presence of excess PnA. Under these concentration conditions, there is only about 5% free *cis*-PnA when the molar ratio of BSA/*cis*-PnA equals 0.25 (assuming binding constants $\geq 5 \times 10^6$ $M^{-1}$ for the tightest five sites) and less free PnA as the BSA is increased. The growth of the molar ellipticity as BSA is increased reflects the reduction of free *cis*-PnA. An analysis of these data indicates that only the first three to four binding sites contribute to the CD.

The magnitude of the peak molar ellipticity is approximately 45 000, corresponding to a value of $\Delta\epsilon$ of 13 or $\Delta\epsilon/\epsilon_{max} = 1.7 \times 10^{-4}$. This is comparable to the values observed for rhodopsin (Crescitelli et al., 1966). For low ratios of *cis*-PnA/BSA the CD spectral peaks coincide with the absorption peaks. The negative CD component at 315–330 nm appears as the second molecule binds. It should be noted that there is a corresponding small shift and broadening of the absorption spectrum (Figure 2) when the mole ratio of either *cis*-PnA or *cis*-EsA to BSA is varied between 1 and 2. These effects are probably explained by an excitonic interaction between the bound polyene chromophores. It is observed that the addition of non-polyene fatty acids to a solution containing 1 mol of *cis*-PnA per mol of BSA does not produce the negative CD. Under these conditions the PnA should be displaced from the tightest binding site into the weaker binding sites.

*Experimental Observation of Tryptophan to Polyene Fatty Acid Energy Transfer.* The absorption spectra of *cis*-EsA and *cis*-PnA overlap the emission spectrum of the tryptophans of BSA (Figure 6). If the distance between the tryptophans and the bound polyene fatty acids is sufficiently small, it is expected that there will be significant quenching of the tryptophan fluorescence on binding. The distance corresponding to 50% energy transfer from tryptophan to *cis*-PnA can be estimated from the spectral properties of these chromophores and an assumed orientation factor of unity. This estimate is 30 to 35 Å (Sklar et al., 1975, 1976). The spectral overlap of *cis*-EsA absorption and BSA tryptophan emission is considerably smaller than for *cis*-PnA, $R_0$ is about 15–20 Å for *cis*-EsA, and consequently less energy transfer is expected.

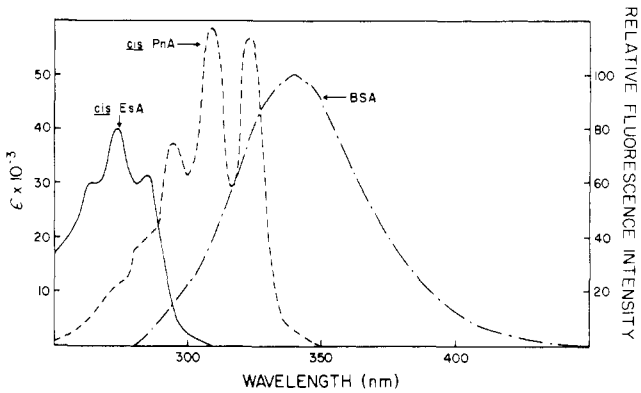


FIGURE 6: The spectral overlap between the absorption of polyene probes and tryptophan emission of BSA. The concentration of the *cis*-EsA solution was $5.9 \times 10^{-6}$ M and contained 0.6 mol of *cis*-EsA/mol of BSA. The concentration of the *cis*-PnA solution was $3.65 \times 10^{-6}$ M and contained 0.77 mol of *cis*-PnA/mol of BSA. Under these conditions it is expected that nearly all of the fatty acid is bound. The uncorrected emission spectrum of BSA was obtained for a sample containing 0.35 mg/mL BSA using excitation at 280 nm (bandwidth 16 nm) and emission slit width of 2 nm.

The decrease in BSA tryptophan fluorescence associated with the binding of *cis*-PnA, *cis*-EsA, and oleic acid is shown in Figure 7. The BSA tryptophan intensity at 340 nm is plotted in Figure 8A as a function of the number of moles of fatty acid added per mole of BSA. The points in this figure have been corrected for the small amount of direct absorption of the excitation light by parinaric acid and the direct absorption of radiated tryptophan fluorescence. This was done by measuring the effect of *cis*-PnA and *cis*-EsA on the fluorescence of solutions of tryptophan and ovalbumin.

It is clear from Figures 7 and 8 that the binding of *cis*-PnA to BSA results in a considerably larger decrease in tryptophan fluorescence than does the binding of oleic acid. We attribute this increase in fluorescence quenching to Förster radiationless energy transfer from the tryptophan to the polyene fatty acid. This energy transfer is demonstrated directly by the fact that the excitation spectrum of the fluorescence of *cis*-PnA bound to BSA (monitored at $\lambda > 440$ nm) has a maximum at 280 nm due to tryptophan absorption. *cis*-EsA is less effective than

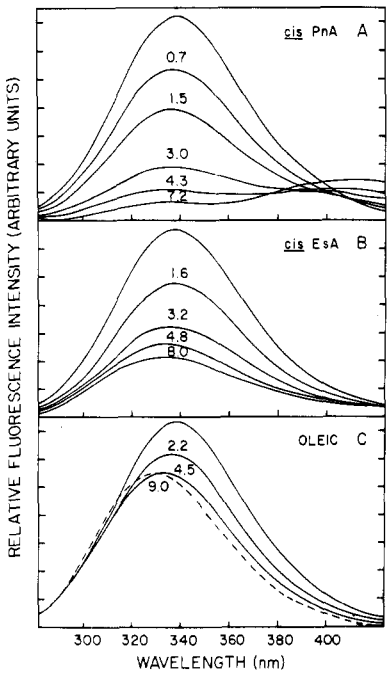


FIGURE 7: The fluorescence emission spectrum of BSA in the presence of *cis*-parinaric acid, *cis*-eleostearic acid, and oleic acid. The BSA concentration of the samples was $3.3 \times 10^{-6}$ M. Measurements used excitation at 240 nm (bandwidth 24 nm). The numbers refer to the ratios of mol of fatty acid/mol of BSA. These spectra are not corrected for inner filter effects.

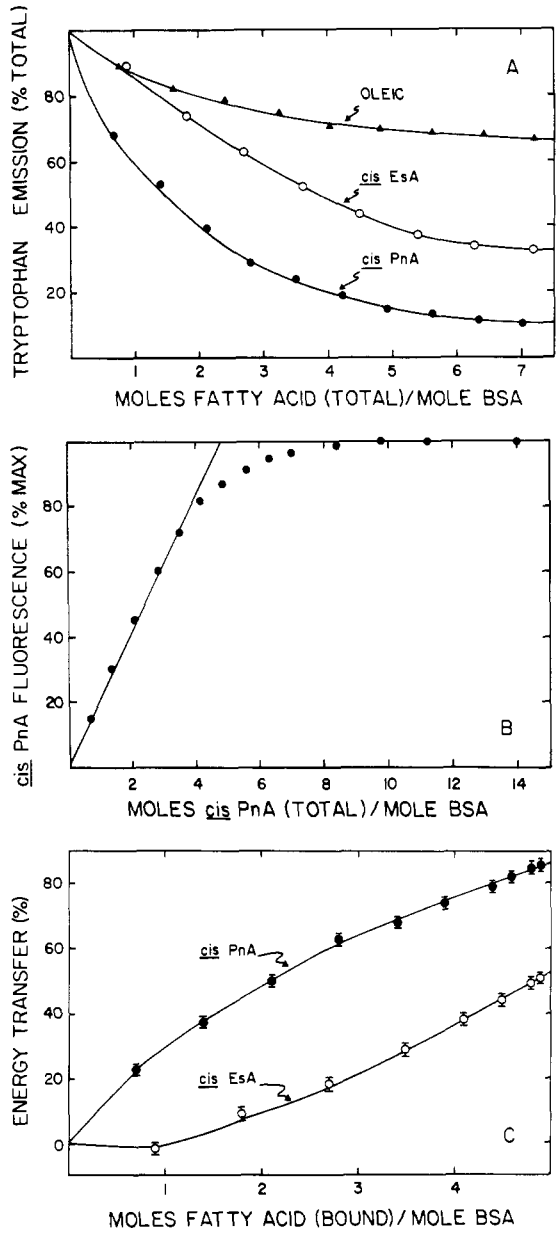


FIGURE 8: Fluorescence energy transfer between BSA and polyene fatty acids. (A) The quenching of tryptophan emission by oleic acid (▲), *cis*-EsA (○), and *cis*-PnA (●). (B) The binding of *cis*-PnA to BSA, as determined by enhanced fluorescence. The BSA concentration was $3.3 \times 10^{-6}$ M. Fatty acids were added as aliquots of ethanolic stock solutions with concentrations of fatty acid $\sim 4 \times 10^{-3}$ M. In A, BSA was excited at 240 nm (bandwidth 24 nm) to avoid direct excitation of *cis*-PnA and to minimize the interference of *cis*-EsA. Emission was at 340 nm (bandwidth 24 nm). Each data point represents an average of at least four determinations and has been corrected for inner and outer filter effects. In B, *cis*-PnA was excited at 325 nm (bandwidth 2 nm) with emission at 420 nm (bandwidth 40 nm). Each data point represents an average of six determinations and has been corrected for the tryptophan contribution. In C, the energy transfer has been corrected for the effect of oleic acid (A) and the assumption of equivalent binding of the fatty acids (B), as described in the text.

*cis*-PnA as a fluorescence quencher when only 1 mol of fatty acid is bound, but for higher mole ratios the incremental quenching is similar for *cis*-EsA and *cis*-PnA (see Figures 8A and 8C).

In order to determine the number of moles of fatty acid bound to BSA, a fluorescence binding curve was determined for *cis*-PnA using the same conditions employed in the tryptophan quenching studies (Figure 8B). The initial linear fluorescence increase extrapolates to a value of approximately 5 mol of *cis*-PnA bound per mol of BSA. The binding affinities of *cis*-EsA and oleate are the same as that of *cis*-PnA to within a factor of two and we therefore use this *cis*-PnA binding curve to estimate the degree of binding of all three fatty acids. Small differences in the binding affinities have no appreciable affect on this binding estimate for $\nu \leq 4$ since the concentration conditions are such that essentially all of the fatty acid is bound.

The total weighted energy transfer efficiency defined by eq 4 in Materials and Methods is related to experimental observations by

$$\overline{T} = 1 - Q(\nu)/Q^{\circ}(\nu) \qquad (11)$$

where $Q(\nu)$ is the quantum yield in the presence of $\nu$ bound acceptors and $Q^{\circ}(\nu)$ is the tryptophan quantum yield in the absence of energy transfer but with the radiative and all other radiationless rates the same. It is clear from the data of Figures 7 and 8 and from the results of other workers (Spector and John, 1968; Morrisett et al., 1975) that the average fluorescence quantum yield of the tryptophans of BSA decreases as oleic acid binds to the protein. A similar decrease in emission intensity is observed with the binding of most long-chain fatty acids (Spector and John, 1968) and is accompanied by a small blue shift (5 nm) in the tryptophan emission spectrum. This decrease in the fluorescence intensity of BSA tryptophan associated with oleic acid binding is not due to Förster energy transfer, but rather to a conformational effect that changes the excited state decay rate ($k_D$ of eq 2). A detailed hypothesis has been proposed (Spector, 1975) to account for these fluorescence intensity and wavelength changes. We will make the assumption that the conformational fluorescence effects that are observed with oleate binding are also present when the polyene fatty acids *cis*-EsA and *cis*-PnA bind to BSA. This seems reasonable in view of the fact that saturated and unsaturated long-chain fatty acids produce similar intensity

changes. The quantity $Q^\circ(\nu)$ in eq 11 will therefore be replaced by $Q(\nu_0)$, the quantum yield of BSA with $\nu_0$ mol of bound oleate. The tryptophan fluorescence intensity data of Figure 8A corrected for binding using 8B and the conformational quenching effect are plotted as the average energy transfer efficiency in Figure 8C.

The total energy transfer efficiency for *cis*-PnA is 86% when about 5 mol of fatty acid is bound. At a similar value of $\nu$ the transfer efficiency for *cis*-EsA is 53%. It is clear, however, that most of this difference is due to the much lower efficiency of quenching of the first mole of *cis*-EsA compared with the first mole of *cis*-PnA. When $\nu = 1$, the average transfer efficiency for *cis*-PnA is 30%, while that for *cis*-EsA is essentially zero. For $\nu > 1$ the differential quenching due to *cis*-PnA and *cis*-EsA is similar even though $R_0$ for *cis*-EsA is much smaller than $R_0$ for *cis*-PnA. It is therefore clear that some of the fatty acids which bind subsequent to the first mole must be quite close to one or both tryptophans.

*Extraction of the Individual Donor Transfer Efficiencies.* Excitation of BSA in the long wavelength tail of the absorption results in a highly polarized fluorescence indicating that the tryptophan residues in BSA have little rotational freedom independent of the overall protein rotation (Weber, 1959). The fluorescence polarization of *cis*-PnA bound to BSA is very high. (The small degree of depolarization leads to an estimated rotational correlation time of 50 ns or longer for the complex.) We conclude that each donor–acceptor pair is characterized by a mutual orientation and distance which are fixed on the time scale of the transfer process. We further assume that each bound acceptor has a unique orientation and distance with respect to the two tryptophan donors.

In order to make a quantitative analysis of this energy transfer data it is necessary to decompose the total transfer efficiency into the components due to the individual tryptophan donors. In order to do this we make use of the analysis presented in Materials and Methods and the experimental observations of Figures 6 and 8C. The basic assumption of this analysis is that the difference between the transfer efficiency observed for *cis*-PnA and *cis*-EsA (Figure 8C) is due to the much lower spectral overlap of *cis*-EsA absorption with BSA tryptophan emission compared with that for *cis*-PnA (Figure 6). It is reasonable to assume that the structural parameters $\kappa_{da}^2$ and $R_{da}$ are very similar for *cis*-EsA and *cis*-PnA in each particular binding site because of the great structural similarity of these two compounds. It is also a reasonable approximation to regard the various acceptors as spectrally identical in that the polyene fatty acid has essentially the same absorption spectrum no matter which site it is bound to. The analysis developed in eq 6–10 is therefore applicable.

The two tryptophans of BSA are probably not spectrally identical (Spector, 1975; Burstein et al., 1973) and therefore the overlap integral ratio $\Gamma$ of eq 6, 8, and 10 may be different for the two donors. However, the values of $\Gamma$ calculated for extreme tryptophan emission spectra are sufficiently similar that a single average value can be used without appreciably changing the quantitative results. Therefore in eq 8 and 10 we set $d = e$ since $d \equiv \Gamma_I$ and $e \equiv \Gamma_{II}$. The numerical value of $\Gamma$ for the total BSA emission is $1.2 \times 10^{-2}$. The quantities $b$ and $c$ ($\overline{T}^A \equiv b \equiv \overline{T}^P$, $\overline{T}^B \equiv c \equiv \overline{T}^E$) are obtained from Figure 8C for a given (integer) value of $\nu$.

It should be noted that there is no operational distinction between tryptophan I and II so far as our analysis is concerned (given that $\Gamma_I = \Gamma_{II}$). For convenience we will define tryptophan I as the donor with the larger transfer efficiency to the fatty acid acceptors. It will be shown below that this designation is unique for all values of $\nu$.

The final quantity needed to evaluate the expressions in eq 10 is $a \equiv f_I$, the relative fluorescence quantum yield of the "first" tryptophan donor in the absence of transfer to acceptors. This quantity is unknown. It seems likely that $f_I$ is in the range 0.3 to 0.7. The average fluorescence quantum yield of the tryptophans of BSA is already abnormally large (0.4) and values of $f_I$ near unity (or zero) would mean that tryptophan I (or II) had a quantum yield near 0.8. For the purposes of our analysis, however, the value of $f_I$ is treated as an unknown and eq 9 and 10 are solved for all values of $f_I$.

In order to make this analysis concrete the case of $\nu = 5$ will be considered in detail. The value of $\overline{T}^P \equiv b$ is 0.86 and $\overline{T}^E \equiv c$ is 0.53 as shown in Figure 8C. The plus root of quadratic eq 9 coincides with the definition of tryptophan I as the one with the highest transfer efficiency. The minus root gives the same numerical results with the labels interchanged. For $f_I$ in the range 0 to 0.5 it is found that the values of the transfer efficiency for donor I to *cis*-PnA and *cis*-EsA exceed unity. For $f_I$ between about 0.87 and unity it is found that the transfer efficiencies for donor II are negative. For $0.55 \leq f_I < 0.85$ all of the transfer efficiencies are between zero and unity and, for the plus root, the transfer efficiency for donor I is much larger than for donor II. The values of the transfer efficiency for donor I to the five *cis*-PnA acceptors obtained with $f_I$ in this allowed range are between 0.993 and unity. For one extreme case ($f_I = 0.55$) we find $T_I^P = 1$, $T_{II}^P = 0.690$, $T_I^E = 0.942$, and $T_{II}^E = 0.0260$. The other extreme case ($f_I = 0.85$) results in $T_I^P = 0.993$, $T_{II}^P = 0.108$, $T_I^E = 0.623$, and $T_{II}^E = 0.001$.

The analysis for lower values of $\nu$ is similar and is shown in Table I. In each case the condition that the transfer efficiencies be between zero and unity limits the permitted range of $f_I$. It should be pointed out that $f_I$ is probably a function of $\nu$ since the conformational fluorescence intensity effect noted above probably affects one of the tryptophans more than the other. The analysis for $\nu = 1$ is based on the assumption that the total quenching due to *cis*-EsA is equal to the uncertainty in the measurement or about 1%. Raising this to as much as 5% makes no important changes in the resulting individual transfer efficiencies. Use of a lower value of $\overline{T}^E$ results in an increased range for $f_I$ and $T_I^P$ such that no information can be extracted from the $\nu = 1$ data. It is clear, however, that the observation of less than 1% transfer to one bound *cis*-EsA is consistent with the data obtained for higher values of $\nu$.

The major conclusion of this analysis is that the energy transfer efficiencies of donors I and II are very different. Essentially all of the quenching due to energy transfer is due to transfer from one of the tryptophans.

*Extraction of Distance Information from the Individual Donor Transfer Efficiencies.* The quantity $T_I^P(\nu)$ is the total efficiency with which $\nu$ bound *cis*-PnA molecules quench the fluorescence of donor I. This may be related to the geometric parameters of the complex using the relations

$$T_d/(1 - T_d) = \sum_{a=1}^{\nu} (R_{da}^\circ/R_{da})^6 \qquad (12)$$

$$R_{da}^\circ = 9.79 \times 10^3 (J_{da} Q_d n^{-4} \kappa_{da}^2)^{1/6} \qquad (13)$$

(Gennis and Cantor, 1972; Bay and Pearlstein, 1963; Dale and Teale, 1970).

The orientation factor $\kappa^2$ in eq 13 is not known for any of the donor–acceptor pairs. In principle limits on $\kappa^2$ could be obtained from polarization measurements of the emission following energy transfer. Unfortunately tryptophan has a very low intrinsic polarization when excited in the higher energy regions of its absorption (Weber, 1959) where the parinaric

TABLE I: Energy Transfer Efficiencies and Allowed Range of the Relative Quantum Yield (in Percent).

| $\nu$ | $\overline{T}^P$ | $\overline{T}^E$ | $f_I$ | $T_I^P$ | $T_{II}^P$ | $T_I^E$ | $T_{II}^E$ |
|---|---|---|---|---|---|---|---|
| 1 | 30 | (1) | 45–0 | 65–100 | 1–30 | 2–51 | 0–0.5 |
| 2 | 50 | 10 | 50–0 | 95–100 | 5–45 | 20–91 | 0–1 |
| 3 | 65 | 20 | 65–20 | 97–100 | 5–56 | 31–94 | 0–2 |
| 4 | 75 | 37 | 75–35 | 98.7–100 | 4–62 | 49–90 | 0–2 |
| 5 | 86 | 53 | 85–55 | 99.3–100 | 11–69 | 62–94 | 0–3 |

TABLE II: The Fluorescence Properties and Energy Transfer Parameters of Tryptophan Residues for Transfer to Polyene Fatty Acids.

| Type[a] | $\lambda_{max}$[b] | $\lambda_{1/2}$[c] | $Q$ | *cis*-PnA | | *cis*-EsA | | $\Gamma_d$[f] |
|---|---|---|---|---|---|---|---|---|
| | | | | $J$[d] | $R_0$[e] | $J$[d] | $R_0$[e] | |
| Buried (I) | 331 | 49 | 0.1 | 187 | 27 | 3 | 13 | 0.016 |
| Surface (II) | 341 | 54 | 0.3 | 126 | 30 | 1.3 | 14 | 0.010 |
| Exposed (III) | 352 | 60 | 0.2 | 65 | 25 | 0.9 | 12 | 0.014 |

[a] Classes I, II, and III of Burstein et al. (1973). [b] Fluorescence emission maximum in nm. [c] Fluorescence spectrum half-width at half-height in nm. [d] Spectral overlap integrals $\times 10^{16}$ cm$^3$ M$^{-1}$. [e] $R_{da}°$ of eq 13 with $n = 1.45$ and $\kappa^2 = 1$. [f] $\Gamma_d$ of eq 6 with $B \equiv$ *cis*-EsA and $A \equiv$ *cis*-PnA. In order to obtain complete spectral curves for the calculation of $J$, solutions of ovalbumin, tryptophan in ethanol, and tryptophan in water were used as approximations to the idealized types I, II, and III, respectively.

acid absorption is small. Even under favorable circumstances the limits imposed on $\kappa^2$ by such experiments are so large that they are not of practical importance for donor–acceptor pairs with fixed mutual orientation (Dale and Eisinger, 1975). A maximum value for $R°$ may be obtained by setting $\kappa^2 = 4$.

The other terms in eq 13 can be determined with reasonable accuracy. The spectral overlap integral for tryptophan emission in BSA and parinaric acid absorption is $1.17 \times 10^{-14}$ cm$^3$ M$^{-1}$. The quantum yield of donor I is given by

$$Q_I = 2\overline{Q}°f_c(\nu)f_I \qquad (14)$$

where $\overline{Q}°$ is the quantum yield of tryptophan in the absence of bound fatty acid (0.40), $f_d$ is the factor representing the conformational effect of fatty acid binding and is determined from the oleic acid curve of Figure 8A, and $f_I$ is the value of the relative fluorescence quantum yield used in the analysis given in the previous section. The refractive index in eq 13 can be determined directly from the observed absorption spectral maximum of *cis*-PnA bound to BSA and the correlation of this absorption maximum with refractive index (Sklar et al., 1977a). The value obtained with this procedure is $n = 1.45$.

The other remaining complication is the decomposition of eq 12 into the components due to the individual acceptors. We may obtain an upper limit for the distance between donor I and one of the $\nu$ bound acceptors by replacing the right-hand side of eq 12 by $\nu$ times the average value of the terms in the sum (since one of the terms must be at least as large as the average value) and by using the maximum value of $R°$ obtained by setting $\kappa^2 = 4$ in eq 13. Thus, for $\nu = 2, f_c(\nu) = 0.8, f_I \leq 0.45$, $R° \leq 38$ Å, $T_I^P \geq 0.95$, and $R \leq 26$ Å for one of the tryptophan donor to *cis*-PnA acceptor distances. For $\nu = 5$ it is found that one of the donor–acceptor distances, $R$, must be less than 23 Å. For an orientation factor of $\kappa^2 = 2/3$ one of the tryptophan to parinaric acid chromophore distances is calculated to be 17 Å. This is probably the best estimate for the actual distance.

A spin-labeled fatty acid with the nitroxide group at C-5 quenches the fluorescence of BSA tryptophans more efficiently than oleic acid or a fatty acid labeled at position C-12 (Morrisett et al., 1975). This indicates that a tryptophan is located within about 12 Å of C-5 of one of the bound fatty acids and closer to C-5 and C-12. Since the polyene chromophore is located near the methyl rather than the carboxyl terminus of the acyl chain, the tryptophan to polyene chromophore distance should be somewhat larger than this 12 Å value, in reasonable agreement with the energy transfer results.

Overall, our results indicate that the first fatty acid binding site of BSA is not near either of the two tryptophans, that a second or subsequent binding site is quite near one, but not both, of the tryptophans and that the other more distant tryptophan is the one most strongly affected by the conformational quenching effect. The proximal and distal tryptophans are designated I and II, respectively. This picture is in substantial agreement with that proposed by Spector (1975) and with the recent structural model proposed by Brown (1976), particularly if we assume that the sequential fatty acid binding occurs to domain III first, followed by binding to domain II. In this scheme we assign tryptophans I and II to those at sequence positions 212 (in domain II) and 134 (in domain I), respectively. This assignment is consistent with results obtained for human serum albumin which is missing the tryptophan in domain I (Berde, Hudson, Simoni, and Sklar, in preparation).

*Discussion of the Generality of Polyene Fatty Acid Spectral Methods.* The study of lipid–protein interactions with polyene fatty acid spectroscopy is of much more general interest than this particular case of BSA. Several points relating to the generality of these techniques will be mentioned here.

The complex induced CD observed for the *cis*-PnA–BSA complex is also observed for human and rabbit serum albumins. A strong entirely negative CD is observed for *cis*-PnA bound to $\beta$-lactoglobulin. Only a weak induced CD occurs with binding to solubilized rat liver microsomal cytochrome P-450 and human serum high-density lipoproteins. It seems clear that polyene fatty acid induced CD will be a useful tool for the study of lipid–protein interactions and the geometry of protein-bound lipids, particularly when combined with the increased sensitivity and information of fluorescence detected CD.

The quenching of tryptophan fluorescence due to energy transfer to polyene fatty acids is also a phenomenon with general applicability. The fluorescence properties of tryptophan residues in proteins vary considerably and it is of some interest to estimate the effect of this variability on the efficiency of quenching by polyene fatty acids. For this purpose

we have used the classification scheme of Burstein et al. (1973) in order to have data corresponding to a reasonable spread of tryptophan types. The spectral properties for three types of tryptophans and the calculated parameters for energy transfer to *cis*-PnA and *cis*-EsA are given in Table II. The major conclusion of this analysis is that the differences in the spectral overlap integral J are sufficiently large for different types of tryptophan donors that this variation must be considered in the quantitative evaluation of fluorescence quenching data.

Energy transfer for membrane bound proteins to polyene fatty acids or polyene labeled lipids in the lipid bilayer matrix is of particular interest because of the possibility of detecting lateral phase separation of the protein component. In this case the orientational motion of the polyene chromophore must also be considered. In a solid phase lipid the polyene chromophore is essentially rigid while in the fluid phase the rotational motion is rapid but constrained in its angular extent (Sklar et al., 1977b).

Acknowledgments

We thank Marianne Petersen, Ruth Records, and Edward Bunnenberg for their contributions to the CD studies, John Dawson for a gift of cytochrome P-450, John Kane for a gift of lipoprotein particles, Charles Berde for helpful discussions, and Carolyn Kobielus, Diane Simoni, and Gretchen Montalbano for assistance in the preparation of the manuscript.

References

Ashbrook, J. D., Spector, A. A., Santos, E. C., and Fletcher, J. F. (1975), *J. Biol. Chem. 250,* 2333.

Bay, Z., and Pearlstein, R. M. (1963), *Proc. Natl. Acad. Sci. U.S.A. 50,* 1071.

Berlman, I. B. (1971), Handbook of Fluorescence Spectra of Aromatic Molecules, 2nd ed, New York, N.Y., Academic Press, p 302.

Brown, J. R. (1976), *Fed. Proc., Fed. Am. Soc., Exp. Biol. 35,* 2141.

Burstein, E. A., Vedenkina, N. S., and Ivkova, M. N. (1973), *Photochem. Photobiol. 18,* 263.

Crescitelli, F., Mommaerts, W. F. H. M., and Shaw, T. I. (1966), *Proc. Natl. Acad. Sci. U.S.A. 56,* 1721.

Dale, R. E., and Eisinger, J. (1975), in Biochemical Fluorescence: Concepts, Vol. 1, Chen, R. F., and Edelhoch, H., Ed., New York, N.Y., Marcel Dekker, p 115.

Dale, R. E., and Teale, F. W. J. (1970), *Photochem. Photobiol. 12,* 99.

Gennis, R. B., and Cantor, C. R. (1972), *Biochemistry 11,* 2509.

Goodman, D. S. (1958), *J. Am. Chem. Soc. 80,* 3892.

Hudson, B. S., and Kohler, B. E. (1974), *Annu. Rev. Phys. Chem. 25,* 437.

Longworth, J. W. (1971), in Excited States of Proteins and Nucleic Acids, Steiner, R. F., and Weinryb, I., Ed., New York, N.Y., Plenum Press, pp 433–434.

Morrisett, J. D., Pownall, J. H., and Gotto, A. M., Jr. (1975), *J. Biol. Chem. 250,* 2487.

Muller, N., and Mead, R. J., Jr. (1973), *Biochemistry 12,* 3831.

Reynolds, J., Herbert, S., and Steinhart, J. (1968), *Biochemistry 7,* 1357.

Sklar, L. A. (1976), Thesis, Stanford University.

Sklar, L. A., Hudson, B. S., Petersen, M., and Diamond, J. (1977a), *Biochemistry 16,* 813.

Sklar, L. A., Hudson, B. S., and Simoni, R. D. (1975), *Proc. Natl. Acad. Sci. U.S.A. 72,* 1649.

Sklar, L. A., Hudson, B. S., and Simoni, R. D. (1976), *J. Supramol. Struct. 4,* 449.

Sklar, L. A., Hudson, B. S., and Simoni, R. D. (1977b), *Biochemistry 16,* 819.

Spector, A. A. (1975), *J. Lipid Res. 16,* 165.

Spector, A. A., Fletcher, J. E., and Ashbrook, J. D. (1971), *Biochemistry 10,* 1232.

Spector, A. A., and John, K. M. (1968), *Arch. Biochem. Biophys. 127,* 65.

Weber, G. (1959), *Biochem. J. 75,* 345.